JOURNAL OF TISSUE ENGINEERING AND REGENERATIVE MEDICINE
J Tissue Eng Regen Med 2016.
Published online in Wiley Online Library (wileyonlinelibrary.com) **DOI:** 10.1002/term.2189

RESEARCH ARTICLE

Modulating cell adhesion to polybutylene succinate biotextile constructs for tissue engineering applications

Viviana P. Ribeiro[1,2], Lília R. Almeida[1,2], Ana R. Martins[1,2], Iva Pashkuleva[1,2], Alexandra P. Marques[1,2], Ana S. Ribeiro[3], Carla J. Silva[3], Graça Bonifácio[4], Rui A. Sousa[1,2], Ana L. Oliveira[1,2,5]* and Rui L. Reis[1,2]

[1]*3B's Research Group – Biomaterials, Biodegradables and Biomimetics, University of Minho, Headquarters of the European Institute of Excellence on Tissue Engineering and Regenerative Medicine, Guimarães, Portugal*
[2]*ICVS/3B's – PT Government Associated Laboratory, Braga/Guimarães, Portugal*
[3]*CeNTI, Centre for Nanotechnology and Smart Materials, V. N. Famalicão, Portugal*
[4]*CITEVE, Technological Centre for Textile and Clothing Industry, V. N. Famalicão, Portugal*
[5]*CBQF–Centre for Biotechnology and Fine Chemistry, Portuguese Catholic University, Porto, Portugal*

Abstract

Textile-based technologies are powerful routes for the production of three-dimensional porous architectures for tissue engineering applications because of their feasibility and possibility for scaling-up. Herein, the use of knitting technology to produce polybutylene succinate fibre-based porous architectures is described. Furthermore, different treatments have been applied to functionalize the surface of the scaffolds developed: sodium hydroxide etching, ultraviolet radiation exposure in an ozone atmosphere and grafting (acrylic acid, vinyl phosphonic acid and vinyl sulphonic acid) after oxygen plasma activation as a way to tailor cell adhesion. A possible effect of the applied treatments on the bulk properties of the textile scaffolds has been considered and thus tensile tests in dry and hydrated states were also carried out. The microscopy results indicated that the surface morphology and roughness were affected by the applied treatments. The X-ray photoelectron spectroscopy and contact angle measurements showed the incorporation of oxygen-containing groups and higher surface free energy as result of the surface treatments applied. The DNA quantification and scanning electron microscopy analysis revealed that these modifications enhanced cell adhesion and altered cell morphology. Generally, sodium hydroxide treatment altered most significantly the surface properties, which in turn resulted in a high number of cells adherent to these surfaces. Based on the results obtained, the proposed surface treatments are appropriate to modify polybutylene succinate knitting scaffolds, influencing cell adhesion and its potential for use in tissue engineering applications.

Received 4 December 2015; Revised 6 February 2016; Accepted 14 March 2016

Supporting information may be found in the online version of this article.

Keywords **biotextile; scaffold; polybutylene succinate; surface modification; tissue engineering; biomedical; knitted structure**

1. Introduction

Fibre-based technologies offer a wide range of possibilities to prepare polymeric porous three-dimensional (3D) biodegradable scaffolds for tissue engineering (TE) applications. Fibre networks with high surface area and interconnectivity are particularly interesting as they facilitate tissue ingrowth and can be produced using textile technologies (Hutmacher, 2000; Salgado *et al*., 2004; Gomes *et al*., 2006; Oliveira *et al*., 2007; Chen *et al*., 2009; Tuzlakoglu and Reis, 2009). These technologies have several advantages such as scale-up to industrial production, superior control over the material design, manufacturing precision and reproducibility (Ramakrishna, 2001; Sumanasinghe and King, 2003, 2005). Furthermore, computerization allows production of predesigned architectures with properties tailored to the final requirements of a targeted medical application (Burns and Snyder, 2009; Inui *et al*., 2010; Liu *et al*., 2010; Shikinami *et al*., 2010). Indeed, some traditional textiles have fulfilled the basic requirements for TE scaffolding, namely biocompatibility, flexibility or strength. In particular, knitted technologies are extremely useful as they present better extensibility and controlled porosity/volume (Wang *et al*., 2011). Few knitted structures from synthetic or natural polymers, alone or combined with other types of biomaterials, have been proposed for the construction of 3D scaffolds to repair and regenerate specific tissues. Xingang and coworkers (Wang *et al*., 2013) developed a well-supported dermal substitute by integrating a poly(L-lactide-co-glycolide) (PLGA) knitted mesh with a collagen–chitosan scaffold. Liu *et al.* (2008) fabricated a silk-based scaffold combining web-like microporous silk sponges with a knitted silk mesh for ligament TE applications. Subsequently, Fan *et al.* (2009) developed a combined scaffold to regenerate the anterior cruciate ligament in a pig model by rolling a micro-porous knitted silk mesh around a braided silk cord. These few cases reveal the versatility of the knitted biotextiles and the rapid advancements in this field.

*Correspondence to: Ana L. Oliveira, CBQF–Centre for Biotechnology and Fine Chemistry, Portuguese Catholic University, Porto, Rua Arquiteto Lobão Vital, Apartado 2511, 4202-401 Porto, Portugal. E-mail: aloliveira@porto.ucp.pt

However, TE is still a new application for textile technology and therefore most of the devices developed are only in the exploratory stage, seeking further development and optimization.

In the present study, it is proposed that this technology can be used to process biodegradable poly(butylene succinate) (PBS) fibres into 3D structures for TE applications. This aliphatic polyester (Figure 1) is obtained from a natural source (Fujimaki, 1998) and because of its superior mechanical and thermal properties, good processability, high chemical resistance and low cost, it has become a competitive material (Kim *et al*., 2006; Phua *et al*., 2012). Recently, it has been proposed for different applications in the medical field (Li *et al*., 2005; Oliveira *et al*., 2008). This polymer has particular advantages when compared with other synthetic polymers, such as polylactic acid (PLA), polyglycolic acid (PGA), polyethylene oxide (PEO) or poly(lactic-coglycolic) (PLGA) (Correlo *et al*., 2005; Oliveira *et al*., 2008). It has a lower melting point (around 114–118 °C) and higher elongation rate at break (Li *et al*., 2005). The hydrolytic etching of the polylactides results in the release of acidic products, which represents a main drawback of these polymers in the biomedical field. In contrast, PBS degradation products are not cytotoxic, making this polyester very attractive for application in TE (Correlo *et al*., 2005; Oliveira *et al*., 2008). It has recently been demonstrated that PBS can be processed into fibrillar knitted structure owing to its low melt flow index (Almeida *et al*., 2013). In addition to the bulk properties, the biocompatibility of such structures is affected by the surface properties, such as surface energy, chemical composition, wettability and roughness. There are a number of approaches that can tailor the surface characteristics of complex shaped 3D structures for TE applications (Pashkuleva and Reis, 2004; Yoo *et al*., 2009). As a biodegradable aliphatic polyester, PBS is particularly susceptible to surface modification (Zhao *et al*., 2008; Liu *et al*., 2009; Martins *et al*., 2010). Plasma and ultraviolet (UV) irradiation are among the techniques used either for surface modification of biomaterials or for activation of the surfaces before grafting with different functional molecules (Liu *et al*., 2011; Li *et al*., 2012). Both methods have been applied to 3D scaffolds and have shown a positive influence on cell adhesion, spreading, proliferation and differentiation (Bullett *et al*., 2004; Safinia *et al*., 2007; Chen and Su, 2011; Wang *et al*., 2011; Zanden *et al*., 2012; Declercq *et al*., 2013). Zhao *et al*. (2008) reported that PBS films functionalized by acrylic acid (AAc) grafting after plasma activation became more wettable and biodegradable. Ultraviolet etching was applied to PBS/chitosan composite scaffolds and significant changes in the surface roughness, wettability and chemistry were observed (Martins *et al*., 2010). Alkaline hydrolysis has also been confirmed as an efficient surface modification technique while also improving the mechanical properties of biocomposite plates of PBS/jute fibres (Liu *et al*., 2009). However, the selection of a proper method to tailor the surface properties of 3D structures is not a straightforward and easy task as the modification may compromise the constructs biofunctionality. Several treatments were therefore explored to modify the surface of PBS knitted structures, namely: wet chemical etching using NaOH; physical etching/oxidation treatment using a UV ozonator; and grafting of carboxylic, phosphonic and sulphonic groups after plasma surface preactivation. The effect of these treatments in terms of early cell adhesion was then evaluated. The work allowed to better understand how the combination of scaffold design and surface modification affect cell adhesion.

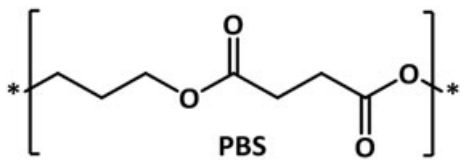

Figure 1. Chemical structure of polybutylene succinate (PBS)

2. Materials and methods

2.1. Production of the textile scaffolds and membranes

Granulated PBS was obtained from Showa Highpolymer Co. Ltd, Tokyo, Japan. The PBS fibres with 36 filaments and an average diameter of 48.9 ± 0.3 μm (Almeida *et al*., 2013) were processed in a multicomponent extruder in mono-component mode (Hills, Inc., West Melbourne, FL, USA). Plain 3D jersey structures of ~0.7 mm were produced through weft knitting using PBS fibres (Tricolab machine; Sodemat, Sturmabteilung, Germany). Scaffolds were washed in a 0.15% (w/v) natural soap aqueous solution for 2 h and then rinsed with distilled water to ensure the full removal of the natural soap. Because some of the characterization techniques used are only applicable to two-dimensional (2D) plan surfaces, PBS membranes were also produced by melt-compression of the granules and modified using the same procedures as the ones used for the 3D structures.

2.2. Surface treatments

2.2.1. Etching with NaOH

The PBS scaffolds were immersed in 0.5 M NaOH solution for 60 min at 30 °C and then washed with distilled water.

2.2.2. Exposure to ultraviolet radiation in an ozone atmosphere (UV/O_3)

The UV/O_3 treatment was performed by exposing the PBS surfaces to 185 nm of UV radiation using a UV/ozone cleaner (ProCleaner™ 220; BioForce Nanosciences, Ames, IA, USA).

DOI: 10.1002/term

2.2.3. Plasma grafting

Plasma treatment was performed using a radio frequency (13.56 MHz) PlasmaPrep5 equipment from Gala Instruments (Berlin, Germany). Samples were exposed to O_2 plasma at 30 W for 15 min. The pressure in the reactor was maintained around 20 Pa by regulating the gas flow. Immediately after plasma treatment, the activated surfaces were immersed in one of the following solutions for 2 h at room temperature, in order to introduce carboxylic, sulphonic or phosphonic groups on the material surface: 5% (v/v) acrylic acid (AAc), 1.1% (w/v) vinyl phosphonic acid (VPA)/2-propanol or 10% (v/v) vinyl sulfonic acid (VSA). Solutions were previously degassed by nitrogen bubbling to avoid the reaction between the induced functional groups and the O_2 present in the solutions. After each reaction, samples were washed with the solvent used to prepare the solutions, distilled water or 2-propanol, followed by drying at 37 °C for 10 min.

2.3. Scanning electron microscopy

Surface morphology was analysed by scanning electron microscopy (SEM) (S360; Leica, Cambridge, UK) before and after the different surface treatments.

Cell adhesion on the surface of materials was also analysed by SEM. After each predefined time-point, the constructs were washed with phosphate buffered saline (Sigma, Sintra, Portugal) and fixed with 2.5% glutaraldehyde (Sigma, Sintra, Portugal) solution in phosphate buffer. Constructs were again rinsed with phosphate buffer and dehydrated using a series of ethanol solutions (30%, 50%, 60%, 70%, 80%, 90% and 100% v/v). Finally, samples were treated with hexamethyldisilazane (HMDS) (Electron Microscopy Sciences, San José, CA, USA) and air-dried overnight at room temperature. All samples were sputter-coated with gold (Sputter 38 Coater SC502; Fisons Instruments, East. Grinstead, UK) before SEM analysis and the micrographs were taken at an accelerating voltage of 15 kV at different magnifications.

2.4. Atomic force microscopy

The surface roughness of the untreated and surface-treated samples was determined by atomic force microscopy (AFM). The analysis was performed on three regions per sample ($5 \times 5\ \mu m^2$) using tapping mode (Veeco, Santa Barbara, CA, USA) connected to a NanoScope III (Veeco, Santa Barbara, CA, USA) with non-contacting silicon nanoprobes (ca. 300 kHz, set point 2–3 V) from Nanosensors (Neuchatel, Switzerland). All images were fitted to a plan surface using the third degree flatten procedure included in the NanoScope software version 4.43r8. The surface roughness was calculated as Ra (mean absolute distance from mean flat surface).

2.5. Mechanical properties measurements

The mechanical properties of the produced PBS textile scaffolds were determined by quasi-static tensile tests (Instron 4505 Universal Machine; Norwood, MA, USA) before and after the different surface modifications. The tensile modulus, ultimate tensile strength and strain at maximum load were measured using a load cell of 1 kN at a crosshead speed of 5 mm/min. The tensile modulus was determined in the most linear region of the stress/strain curve using the secant method. Both dried and hydrated samples were tested. The tests with dried samples were conducted at 25 °C and 50% humidity. Hydrated samples were prepared by immersion in phosphate buffered saline at pH of 7.4 for 3 days. Five samples with dimensions of 15 × 40 mm were analysed per condition.

2.6. Contact angle and surface energy analysis

The wettability of the untreated and modified surfaces was assessed by contact angle (θ) measurements. The static contact angle measurements were obtained by the sessile drop method using a contact angle meter OCA15 + with a high performance image processing system (DataPhysics Instruments, Filderstadt, Germany). The liquids used [H_2O and CH_2I_2, 1 μl, high-pressure liquid chromatography (HPLC) grade] were added by a motor-driven syringe at room temperature. Two samples for each condition were used and five measurements were carried out for each sample. The surface free energy (γ) of the treated and untreated samples was calculated using the Owens, Wendt, Rabel and Kaelble (OWRK) equation (Kaelble, 1970; Altman *et al*., 2003).

2.7. X-ray photoelectron spectroscopy

X-ray photoelectron spectroscopy (XPS) analysis was performed to characterize the surface elemental composition of the modified and unmodified samples using a K-Alpha ESCA instrument (Thermo Scientific, Waltham, MA, USA). Monochromatic Al-Kα radiation ($h\nu$ = 1486.6 eV) was used to perform the XPS measurements and the photoelectrons were collected from a take-off angle of 90° relative to the samples surface. The spectrometer was operated in a constant analyser energy (CAE) mode with 100 eV pass energy for the survey spectra and 20 eV pass energy for the high-resolution spectra. The binding energies positions were referenced to the C1s peak on unsputtered surfaces. Charge referencing was adjusted by setting the lower binding energy of the C1s hydrocarbon peak at 285.0 eV. An electron flood gun was also applied to minimize surface charging. Charge compensation was performed by overlapping the C1s signal before and after each experiment. The overlapped peaks were resolved into their individual components by using the XPSPEAK 4.1 software. The atomic concentrations were determined from the XPS peak areas using the Scofield sensitivity factors. A linear background was selected as subtraction technique. Initially, a Gaussian fitting was performed using fixed parameters for full width at half maximum (FWHM) and the peak positions (i.e. only the peak area was not constrained). After this initial fitting, all

DOI: 10.1002/term

parameters were set as free and a new fitting was performed to obtain the reported values.

2.8. Cell culture

A mouse fibroblast cell line (L929), acquired from the European Collection of Cell Cultures (ECACC UK), was used to assess the effect of the applied surface modifications on cell adhesion. For that purpose, materials were cut into 16 mm diameter discs, and immobilized into the bottom of 24-well culture plates (BD Biosciences, San Jose, CA, USA) using CellCrown® inserts (Scaffdex, Tampere, Finland). Cells were grown as monolayer cultures in Dulbecco's Modified Eagle's Medium (DMEM; Sigma, Sintra, Portugal) supplemented with 10% fetal bovine serum (FBS; Biochrom, Berlin, Germany) and 1% antibiotic–antimycotic solution (Thermo Scientific, Waltham, MA, USA). At confluence cells were detached from the culture flasks using trypsin (Sigma), centrifuged, resuspended in DMEM and seeded into the scaffolds at a density of 30 000 cells/sample. The constructs were incubated at 37 °C, 5% CO_2 and 95% humidity, for 1, 5 and 24 h. Tissue culture polystyrene (TCPS; Sarstedt, Nümbrecht, Germany) coverslips and PBS membranes were used as control surfaces.

2.8.1. Quantification of DNA

At the different time-points the L929 cell number on the constructs developed was indirectly assessed using a fluorometric double-strand DNA quantification kit (PicoGreen; Thermo Scientific, Waltham, MA, USA) following the manufacturer's instructions. After each time-point, constructs were carefully rinsed twice with phosphate buffered saline and transferred into 1.5 ml microtubes containing 1 ml of ultrapure water to induce an osmotic shock. Constructs were kept at −80 °C until further analysis. Before quantification of dsDNA, samples were thawed and sonicated. A PicoGreen solution was mixed with the samples and the standards (ranging from 0 to 2 μg/ml) in a 200:1 ratio and placed into opaque 96-well plates. Each sample or standard was made in triplicate. After 10 min of incubation in the dark, the fluorescence was read into a microplate Enzyme-Linked Immunosorbent Assay (ELISA) reader (BioTek, Winooski, VT, USA) at 485 nm excitation/528 nm emission. To exclude autofluorescence, samples without cells subjected to the same culture conditions were analysed using the same procedure.

2.9. Statistical analysis

All the numerical results are presented as mean ± standard deviation (SD). Statistical tests were performed with GraphPad Prism 5.0 (GraphPad Software, La Jolla, CA, USA). A one-way ANOVA analysis of variance was used to evaluate the AFM, tensile tests and contact angle results, using the Tukey's method as a *post-hoc* pairwise comparison test. Statistical analysis of DNA quantification, obtained from three independent experiments with three samples analysed for each time-point in every experiment, was determined with a two-way ANOVA test followed by Bonferroni's as multiple comparison analysis method. The significance levels are designated as $*p$ 0.05, $**p$ 0.01 and $***p$ 0.001.

3. Results and discussion

The surface design of scaffolds for TE applications is a great challenge but also an extraordinary opportunity since slight changes in the surface chemistry and/or topography can significantly improve the biological performance without changing the bulk properties. In the case of fibres, surface modification is particularly important since there is a great surface area with respect to the total volume of material, which may involve higher effects in terms of biological response.

3.1. Surface morphology and topography

The morphology of the 3D structures and the surface of the fibres were analysed by SEM. Figure 2 presents the micrographs of top (Figure 2a) and bottom (Figure 2b) sides of the PBS knitted structure. The higher magnification micrographs (Figure 2c–h) show the fibres of the top side before and after the different surface treatments.

The unmodified PBS fibres presented a smooth surface without visible pores or defects (Figure 2c). The SEM images of the modified fibres revealed irregularities on their surface induced by all the treatments (Figure 2d–h). Among the different modifications, plasma/VSA exposure seemed to affect the fibres surface most (Figure 2h). When a polymer surface is treated by plasma and subjected to chemical surface functionalization, surface etching can also occur. In fact, chemical surface modification is usually associated with changes in the surface topography/morphology (Lopez-Perez *et al*., 2010). Zhao *et al*. (2008) reported that PBS films functionalized by AAc plasma grafting presented a typical biodegradation pattern with micro-cracked and fragmented surfaces. The surface modification by NaOH has also been reported to induce significant changes in the surface properties of jute fibres in PBS–jute fibre biocomposites (Liu *et al*., 2009). Fibres presented a rougher morphology induced by a decrease of the surface impurities, which is in agreement with the observations in the present study (Figure 2d).

The PBS membranes were analysed by AFM to indirectly characterize the influence of the different surface modifications on the PBS fibres roughness (i.e. the extent of etching). The AFM images of untreated and surface-modified PBS membranes are shown in Figure 3 and the obtained average roughness is presented in Figure 4.

Consistent with the results obtained by SEM analysis, the surface topography of PBS membranes was also affected by the applied treatments (Figure 3b-f). As expected, the chemical etching by NaOH had the most significant effect on the membrane topography, resulting in a

DOI: 10.1002/term

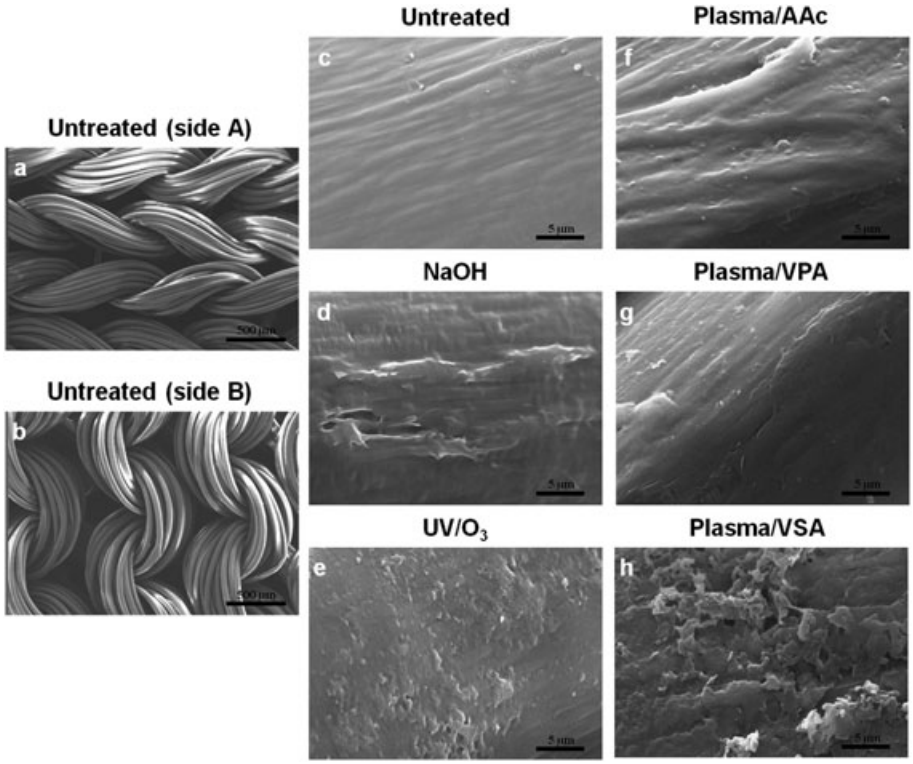

Figure 2. Scanning electron micrographs of polybutylene succinate (PBS) knitted constructs: (a) top and (b) bottom sides of the structure and magnifications of the fibres (side A), (c) before and (d–h) after the surface treatments. AAc, acrylic acid; VPA, vinyl phosphonic acid; VSA, vinyl sulphonic acid; UV/O_3, ultraviolet radiation exposure in an ozone atmosphere

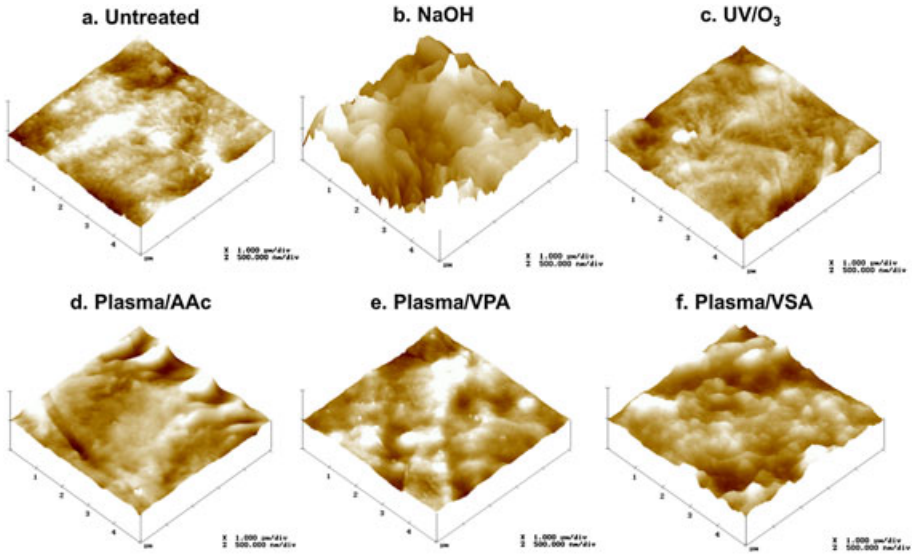

Figure 3. Atomic force microscopy images of the polybutylene succinate (PBS) membranes (a) before and (b–f) after the different surface treatments. AAc, acrylic acid; VPA, vinyl phosphonic acid; VSA, vinyl sulphonic acid; UV/O_3, ultraviolet radiation exposure in an ozone atmosphere

significantly rougher ($p < 0.05$) surface (Figure 4). The results obtained are in agreement with those obtained by Zeronian and Collins (1989), that showed that the surface topography of polyester fibres became rougher after the alkali treatment with NaOH. Martins *et al.* (2010) also observed that the treatment of PBS/chitosan composite scaffolds by UV irradiation with different parameters also increased the surface roughness of the scaffolds by selective etching of the PBS external layer.

3.2. Mechanical properties

Almeida *et al.* (2013) previously demonstrated that PBS knitted structures present water sorption ability. Therefore, it is also important to evaluate the eventual effect of the proposed treatments on the bulk properties of the fibre constructs. Quasi-static tensile tests were performed in the longitudinal direction before and after treatment (Figure 5).

DOI: 10.1002/term

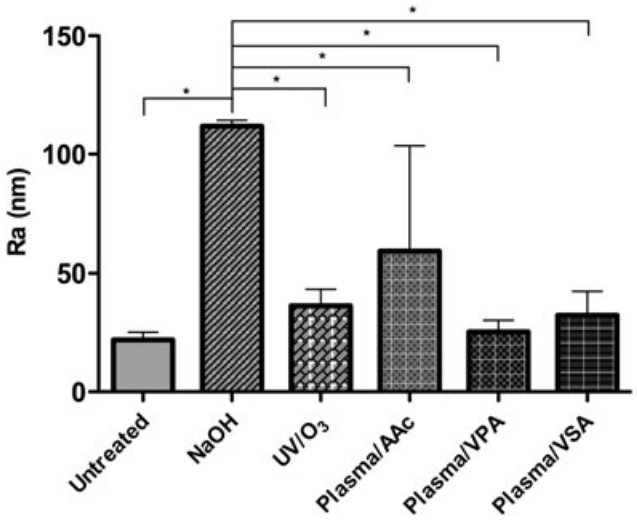

Figure 4. Average roughness (Ra) of the polybutylene succinate (PBS) membranes before and after the different surface treatments. AAc, acrylic acid; VPA, vinyl phosphonic acid; VSA, vinyl sulphonic acid; UV/O_3, ultraviolet radiation exposure in an ozone atmosphere; $*p < 0.05$

Considering that PBS is a semi-crystalline polymer constituted by linear chains, the obtained mechanical properties revealed the typical behaviour of a rigid thermoplastic (Correlo *et al*., 2010). Except for the plasma/VSA treatment, all the applied treatments induced some changes in the scaffolds' mechanical performance (Figure 5), revealing that the treatments applied were not only confined to surface modifications. When comparing the untreated and the surface-treated scaffolds in the dry state, a significantly higher maximum strength (Figure 5a) was obtained for samples treated with plasma/VPA ($p < 0.001$). A greater effect of plasma grafting was also observed on tensile modulus results (Figure 5b), revealing significantly higher levels on samples treated with plasma/AAc ($p < 0.001$) and plasma/VPA ($p < 0.05$), in comparison with the untreated ones. By analysing the strain at maximum load, it was possible to observe that no significant changes were detected between the untreated samples and all the surface-modified samples (Figure 5c). The NaOH-treated samples presented no significant differences in tensile properties in the dry state compared with the untreated surfaces, which is in agreement with the results of Zeronian and Collins (Z1989) who found that the surface treatment of polyester fibres with NaOH did not affect the tenacity of the hydrolyzed products. Even so, a tendency for a decrease in the maximum strength (Figure 5a) and strain at maximum load (Figure 5c) was observed for alkali-treated samples compared with untreated ones. The results presented by Ellison *et al*. (1982) also showed that polyester fibres became more brittle after the reaction with NaOH, presenting an ultimate stress and extension at break significantly lower than the untreated control fibres. This might be explained by the preferable etching of the amouphous regions of the polymer, which are responsible for the ductility component of the polymer. Therefore, it is likely that after the alkali treatment the mechanical properties are mainly attributed to the crystalline domains of the polymer (Cho *et al*., 2001). The analysis of the mechanical properties of the structures in the dry state is important to determine their behaviour at the time of implantation. However, as the scaffolds are expected to be used in a hydrated environment, the mechanical behaviour was also tested in the wet state. A significantly higher strength (Figure 5d) was obtained for samples treated with NaOH ($p < 0.001$) and plasma/VPA ($p < 0.01$) in comparison with the untreated samples. The wet samples treated with NaOH also presented a significantly higher ($p < 0.001$) tensile modulus (Figure 5e) when compared with the untreated ones. An opposite effect was observed for the UV/O_3-treated ($p < 0.001$) samples (Figure 5d,e). The hydration process induced a significantly lower strain at maximum load (Figure 5f) on samples modified by UV/O_3 ($p < 0.01$) and plasma/AAc ($p < 0.05$). The hydration of the polymer fibres might explain the different mechanical behaviours induced by the treatments, owing to increased mobility of molecular chains (Dhakal *et al*., 2007).

3.3. Surface wettability and composition

There are no direct methods to measure the surface energy of scaffolds. However, a number of indirect empirical and semi-empirical methods have been developed based on contact angle measurements (Chan, 1994; Ratner, 1996). The surface energy (γ_s) of PBS samples and the respective polar interactions (γ_p) and dispersion forces (γ_d) were calculated by the OWRK (Owens, Wendt, Rabel and Kaeble) model. The water contact angle values measured for untreated and treated surfaces are presented in Figure 6 and the respective polar and dispersive components of the surface energy are shown in Table 1.

The untreated PBS surfaces presented a rather hydrophobic character with a contact angle of about 106°, consistent with previously reported values for this polyester (Coutinho *et al*., 2008; Zhao *et al*., 2008; Martins *et al*., 2010). A significant decrease ($p < 0.05$, $p < 0.001$) in water contact angle values (Figure 6) was obtained after all surface treatments, except for plasma/VSA-treated samples, which surprisingly presented a significantly higher ($p < 0.05$) water contact angle when compared with the untreated samples. These results indicate that those treatments resulted in more hydrophilic surfaces. As expected, an increase of the surface energy was obtained after all the treatments (Table 1). In case of NaOH, plasma/AAc and plasma/VPA surface treatments, mainly the polar component contributed to the increase in surface energy. In contrast, the increase in surface energy of UV/O_3-treated surfaces was dependent on the increase in the dispersive component. Previous works have demonstrated that the surface modification of PBS-based structures by plasma etching (Coutinho *et al*., 2008), plasma/AAc grafting (Zhao *et al*., 2008) and UV laser processing (Martins *et al*., 2010) also induced a significant decrease in the water contact angle values, enhancing the hydrophilic character of the surfaces. The increased

DOI: 10.1002/term

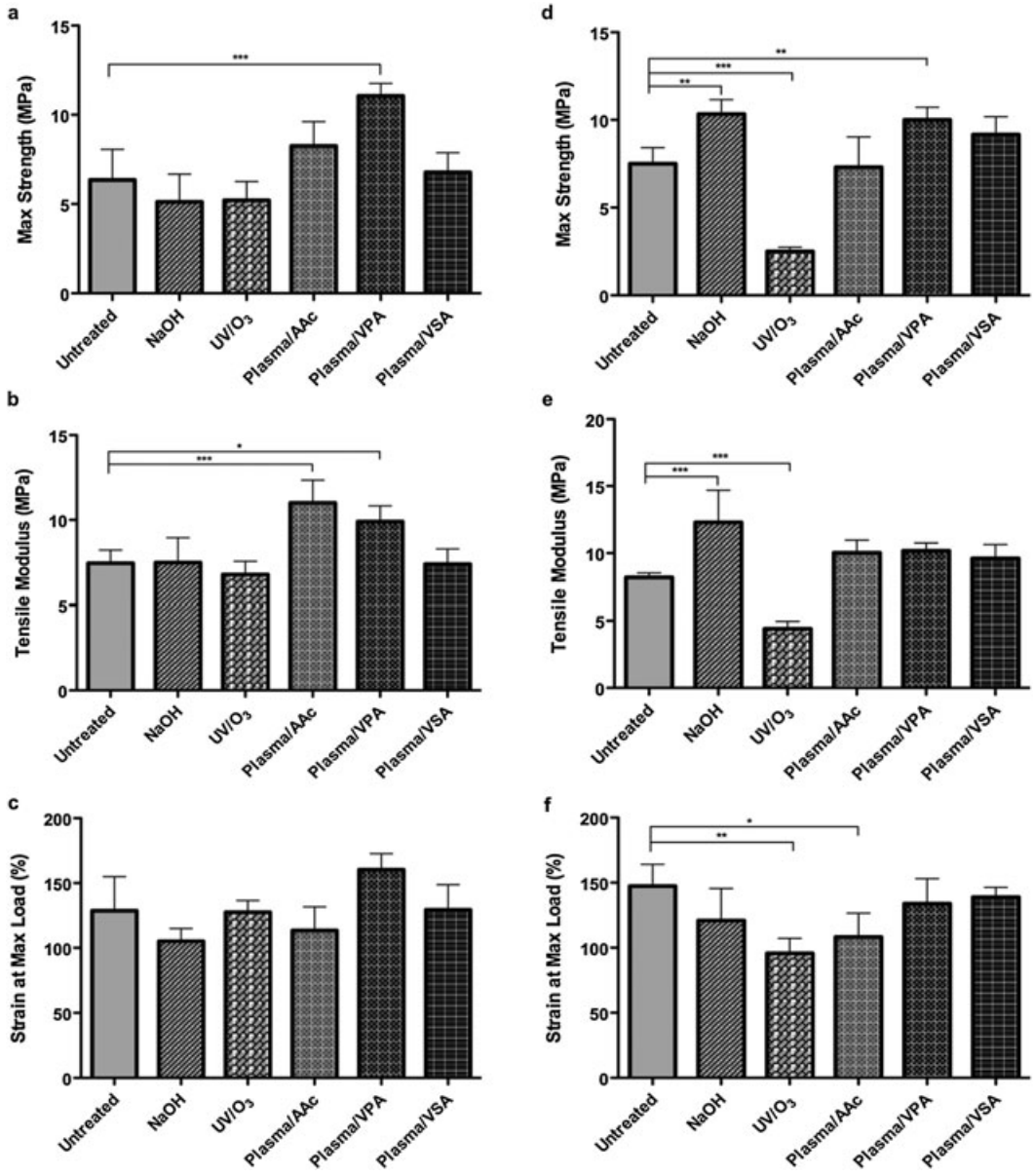

Figure 5. Effects of the different surface modifications on maximum strength (MPa), tensile modulus (MPa) and strain at maximum load (%) obtained for polybutylene succinate (PBS) textile matrices at (a–c) dry (25 °C) and (d–f) hydrated state (isotonic phosphate-buffer saline solution; 37 °C), in the longitudinal direction. AAc, acrylic acid; VPA, vinyl phosphonic acid; VSA, vinyl sulphonic acid; UV/O_3, ultraviolet radiation exposure in an ozone atmosphere; $^*p < 0.05$; $^{**}p < 0.01$; $^{***}p < 0.001$

wettability reached after the plasma treatment and AAc grafting was attributed to functionalization with the hydrophilic groups (−COOH) (Zhao *et al*., 2008). A possible explanation for the results obtained is that most probably the Wenzel effect was occurring. This model describes a homogeneous wetting regime where the spaces of rough surfaces are completely filled by the water. Therefore, a greater roughness results in higher volumes of water (Wenzel 1936).

The surface chemical composition and atomic ratios of PBS samples before and after the different surface treatments were analysed by XPS to complement the surface analysis. Data are summarized in Table 2.

The XPS spectrum of untreated polyester confirms the presence of C (78.8 atom%) and O (17.9 atom%). Some other elements were also detected at a lower percentage (≤ 1) in the atomic composition of the PBS surface (see the Supplementary material online, Figure S1). As can be seen from Table 2, the theoretical oxygen/carbon ratio is higher than that measured for the untreated textile structures. The different measured composition might be explained by possible surface contaminations or by the reorganization/motility of the polymer chains as a result of the processing conditions, which has been observed and described previously (Pashkuleva *et al*., 2008). After the surface treatment the oxygen content for all treated samples increased (Table 2) and two additional peaks appear in the survey spectrum of the sample treated by plasma and VPA grafted (see the Supplementary material online, Figure S2). These peaks were assigned to P2p (133 eV) and P2s (190 eV) and confirmed the successful grafting with VPA. Surprisingly, no sulphur was detected in the survey spectrum of the VSA grafted sample. A possible reason could be the very low amount of the sulphur

DOI: 10.1002/term

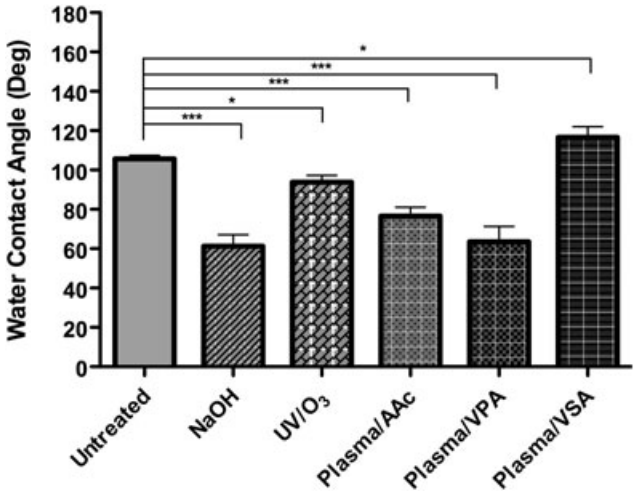

Figure 6. Water contact angle values obtained for the untreated and treated polybutylene succinate (PBS) surfaces. AAc, acrylic acid; VPA, vinyl phosphonic acid; VSA, vinyl sulphonic acid; UV/O_3, ultraviolet radiation exposure in an ozone atmosphere; *$p < 0.05$; ***$p < 0.001$

Table 1. Contact angle values (θ) and surface energy calculations (γ_s) of untreated and surface-treated polybutylene succinate (PBS) samples

Treatment	Contact angle (θ)		Dispersive component (mN/m)	Polar component (mN/m)	Surface energy (mN/m)
	H_2O	CH_2I_2	γ_s^d	γ_s^p	$\gamma_s(\gamma_s^d + \gamma_s^p)$
Untreated	105.7 ± 1.8	70.9 ± 3.9	22.11 ± 0.0	0.15 ± 0.0	22.3 ± 0.0
NaOH	61.3 ± 5.8	43.3 ± 4.9	28.68 ± 0.3	16.85 ± 0.61	45.5 ± 0.68
UV/O_3	93.7 ± 3.4	43.0 ± 5.8	37.2 ± 0.68	0.79 ± 0.36	37.98 ± 0.77
Plasma/AAc	76.6 ± 4.6	55.7 ± 7.0	23.34 ± 0.04	8.58 ± 0.01	31.92 ± 0.04
Plasma/VPA	63.5 ± 7.8	39.7 ± 2.6	29.87 ± 0.25	16.49 ± 0.51	46.36 ± 0.57
Plasma/VSA	116.6 ± 5.5	63.0 ± 4.0	30.28 ± 0.75	0.27 ± 0.27	30.55 ± 0.8

AAc, acrylic acid; VPA, vinyl phosphonic acid; VSA, vinyl sulphonic acid; UV/O_3, ultraviolet radiation exposure in an ozone atmosphere.

Table 2. Chemical composition and O/C atomic ratio of unmodified and surface-modified polybutylene succinate (PBS) samples determined by X-ray photoelectron spectroscopy

Modification	O (atom%)	C (atom%)	S (atom%)	P (atom%)	O/C ratio	Theoretical O/C
Untreated	17.9	78.8	–	–	0.23	0.58
NaOH	25.6	71.4	–	–	0.36	
UV/O_3	20.0	64.4	–	–	0.31	
Plasma/AAc	22.2	60.9	–	–	0.37	
Plasma/VPA	25.4	71.2	–	0.3	0.36	
Plasma/VSA	23.6	70.0	–	-	0.34	

AAc, acrylic acid; VPA, vinyl phosphonic acid; VSA, vinyl sulphonic acid; UV/O_3, ultraviolet radiation exposure in an ozone atmosphere.

present on the surface (i.e. below the detection limit of the instrument). Notably, in the high-resolution S2p spectrum a very low signal at 168.7 eV corresponding to SO_2/SO_3-bound sulphur was observed (see the Supplementary material online, Figure S4).

Additional details about surface chemical composition were obtained from the high-resolution spectra of C1s (Figure 7). As expected, the C1s core level spectrum of untreated PBS (Figure 7a) is composed of three components: the peak at 285.0 eV was assigned to the C–H/C–C chemical bonds of the PBS backbone, the second peak is centred at 286.4 eV and was assigned to C–O bonds and finally, the peak at 289.1 eV corresponded to O–C = O ester groups (Figure 1). No additional components were detected after the treatment with NaOH (Figure 7b). However, the relative intensity of the peaks at 286.4 eV and 289.1 eV (i.e. oxygen bound C) is higher, indicating hydrolytic surface etching. This result is consistent with the data obtained from AFM and contact angle analysis. In the case of the UV/O_3 treatment (Figure 7c) and AAc grafting (Figure 7d) a new component in the C1s spectra appears at 292.4 eV. This peak was associated with the presence of a new functionality introduced by those treatments, namely O–C(=O)–O. As the untreated PBS, the C1s high resolution spectra of plasma treated PBS grafted with VPA (Figure 7e) and VSA (Figure 7f) is composed by three components. The characteristic *C*-PO_3 and *C*-SO_4 signals were expected with low intensity, around 287.5 eV and 287.9 eV, respectively (they are overlapped by the C–O signal). As can be seen from Figure 7e,f the FWHM is wider and its area bigger when compared with the untreated PBS, confirming the overlapping. The P2p high-resolution spectrum for VPA grafted PBS (see the Supplementary material online, Figure S3) showed a single peak centred at 133.4 eV, assigned to the phosphonic species. The observed FWHM for this signal is wide as can be expected for P2p, as this signal corresponds to P2p1/2 and P2p3/2 core-line doublets.

3.4. Cell adhesion and morphology

The scaffolds' surface properties are recognized as dramatically influencing cell behaviour (Craighead *et al.*, 2001; Lim and Donahue, 2007). The DNA quantification (Figure 8A) was performed to evaluate the effect of the different surface modifications on the number of adhered cells over 24 h of culture. Cell adhesion on PBS membranes was compared with the 3D untreated textile surfaces, revealing no significant differences over the culture period. Comparing the DNA values obtained for the modified and the untreated textile scaffolds, the results showed that after 1 h of culture the L929 cells adhered in comparable amounts to the different surfaces. Moreover, significantly higher DNA values were obtained for all the modified surfaces after 5 h ($p < 0.01$, $p < 0.001$) and 24 h ($p < 0.001$) of culture, in comparison with the untreated ones, except for the UV/O_3 surface-treated scaffolds.

The scaffolds' surface properties not only can influence cell adhesion but also how cells further interact with the surface (Stevens and George, 2005). The influence of the surface treatments applied on cell morphology was visualized by SEM. The micrographs obtained (Figure 8B) show that fibroblast morphology was altered according to the modification applied, especially after 24 h of culture. Cells cultured on PBS membranes and on the untreated PBS textile structures presented a similar morphology. As expected, a round morphology was observed on both surfaces after 1 h of culture (Figure 8Ba,d). After 5 h (Figure 8Bb,e) some cells presented cytoplasmic

DOI: 10.1002/term

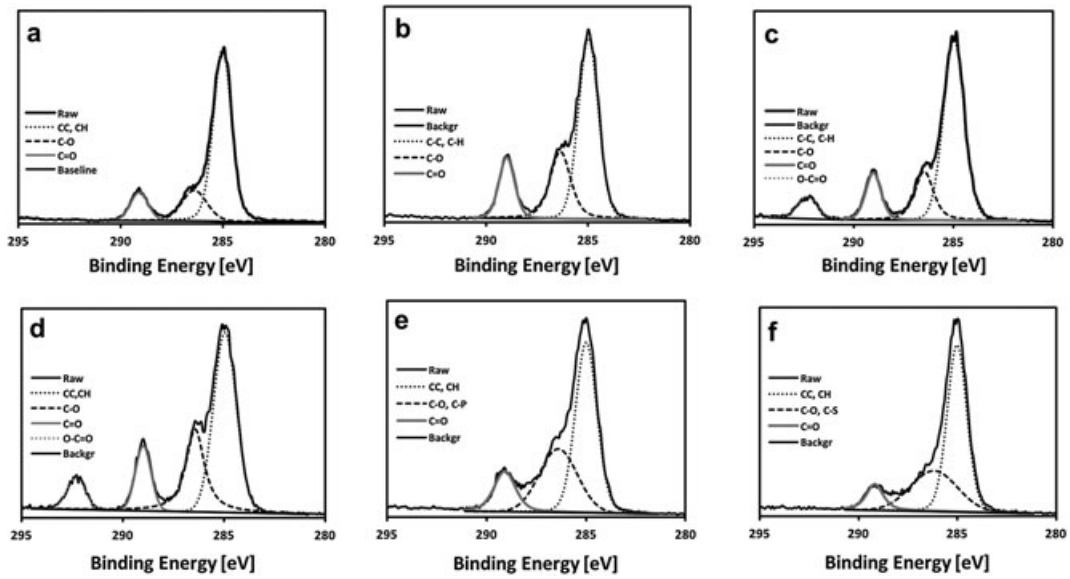

Figure 7. The C1s core level spectra of polybutylene succinate (PBS) (a) before and after modification with (b) NaOH, (c) ultraviolet radiation exposure in an ozone atmosphere and surface activation with plasma and grafting of (d) acrylic acid, (e) vinyl phosphonic acid and (f) vinyl sulphonic acid

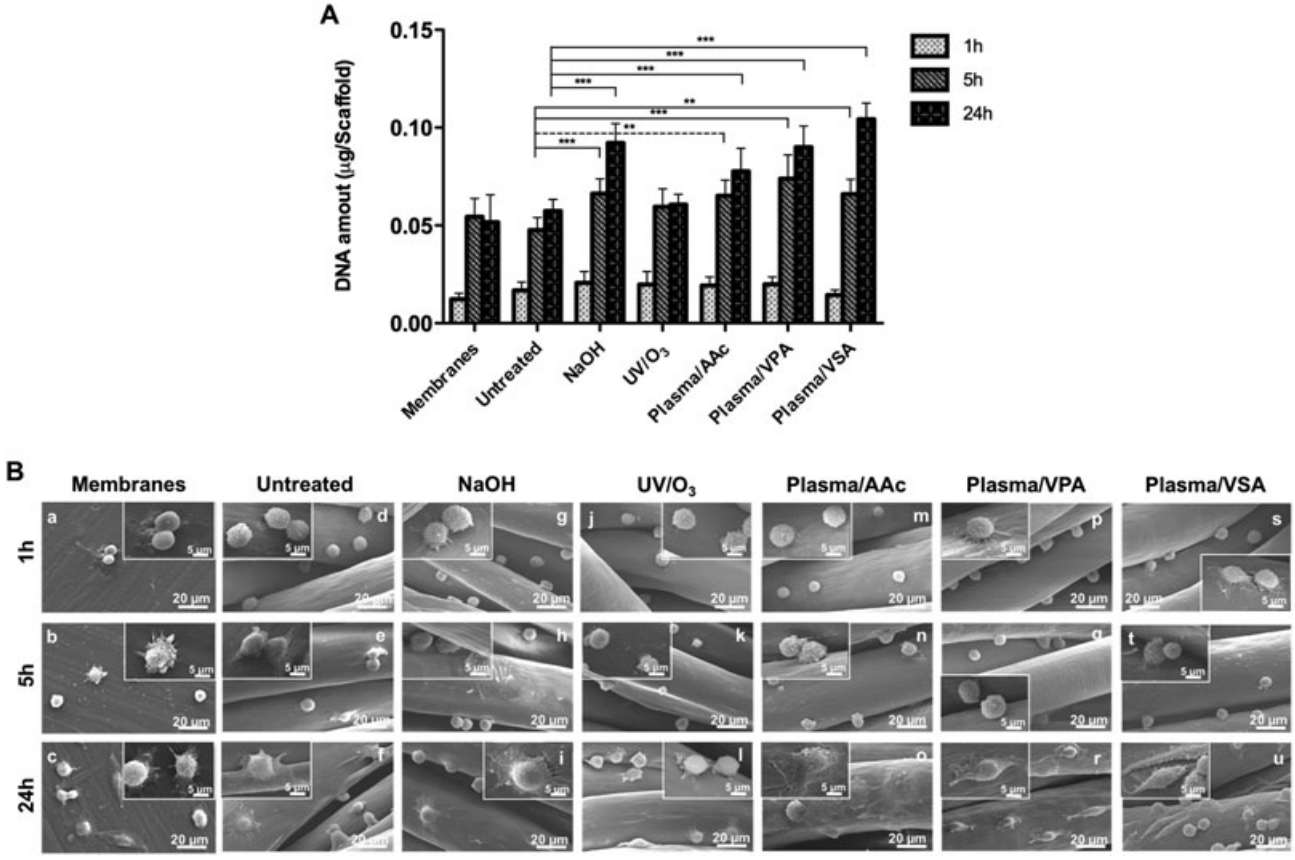

Figure 8. (A) DNA quantification of L929 cells, corresponding to the number of adhered cells on the membranes, untreated and surface-treated polybutylene succinate (PBS) textile scaffolds after 1, 5 and 24 h of culture ($^{**}p < 0.01$, $^{***}p < 0.001$). (B) Scanning electron micrographs of L929 fibroblast-like cells cultured on (a–c) PBS membranes, (d–f) untreated PBS textile scaffolds and surface-treated PBS textile scaffolds: (g–i) NaOH; (j–l) ultraviolet radiation exposure in an ozone atmosphere (UV/O_3); (m–o) plasma/acrylic acid (AAc); (p–r) plasma/vinyl phosphonic (VPA); (s–u) plasma/vinyl sulphonic acid (VSA), for 1 h (a,d,g,j,m,p,s), 5 h (b,e,h,k,n,q,t) and 24 h (c,f,i,l,o,r,u) of culture

projections and after 24 h of culture these processes were even more pronounced, with some elongated cells adhering to the surface (Figure 8Bc,f). Cell morphology on surfaces treated with NaOH and UV/O_3 was similar to that observed on the unmodified textile structures (Figure 8Bg–l). The plasma/AAc grafted PBS fibres

DOI: 10.1002/term

(Figure 8Bo) presented the highest degree of cell spreading after 24 h of culture compared with the remaining surface treatments. On the plasma/VPA (Figure 8Br) and plasma/VSA-treated (Figure 8Bu) surfaces cells presented the typical spindle-like fibroblast morphology, showing their filopodia formation.

It should be noted that the surface properties dictate the very first events occurring when the material contacts with the biological environment. According to earlier studies (Anselme 2000; Mitchell *et al.*, 2005; Coutinho *et al.*, 2008) materials with high surface energy promote faster cell adhesion than low surface energy surfaces. These observations are in accord with our results, as all treated surfaces presented higher surface energy values (Table 1) compared with the untreated ones. Notably, the surface treatment with NaOH and plasma/VPA resulted in the lower contact angle values and higher surface energy, which indicates a higher hydrophilicity of these surfaces that positively affected cell adhesion, as observed from DNA analysis. Moreover, the highest roughness measurements (Figure 4) and oxygen content (Table 2) on NaOH-treated surfaces also corroborate these observations. UV/O_3 surface modification was the only treatment that did not induced significant changes in cell adhesion (Figure 8A), compared with the untreated textile surfaces. This is in accord with a previous work that also reported similar cell adhesion in untreated and UV laser-treated PBS/chitosan composite scaffolds, after 24 h of culture (Martins *et al.*, 2010). The effect of the surface modifications on cell morphology was more pronounced after 24 h of culture (Figure 8Bi,l,o,r,u) and plasma/AAc surface treatment induced the highest effect on cell spreading, represented by the total elongation of cells on the fibres with evident lamellipodia formation (Figure 8Bo). These effects are a consequence of the textiles' surface activation by the plasma treatment followed by the introduction of negatively charged carboxylic functional groups, as confirmed by the detailed surface chemical composition spectra presented in Figure 7d, where a new peak (O–C(=O)–O) in the C1s spectra was associated with the new functionality introduced by the AAc treatment (Delaittre *et al.*, 2012). Moreover, an increase in the surface roughness, as confirmed by AFM (Figure 4), has provided a higher contact area available for cell adhesion. Plasma-induced polymerization of AAc (Park *et al.*, 2007), VPA and VSA (Lopez-Perez *et al.*, 2010) have already proved to be effective treatments for improving cell attachment and spreading. In a different study, the treatment of chitosan/PBS blends by plasma etching also induced a higher degree of cell spreading, creating more adhesion points to the surfaces (Coutinho *et al.*, 2008). The present morphological results do not follow previous reports in the literature showing that the NaOH (Gao *et al.*, 1998) and UV irradiation (Pashkuleva *et al.*, 2010) surface treatments improved cell spreading over the surface of different polymers. Thus, we can speculate that in these cases other parameters in the scaffolds composition may be more influential in cell morphology than the modifications introduced.

4. Conclusions

PBS is a highly promising biodegradable aliphatic polyester for applications in the medical field. Our group was first to develop PBS biotextiles as scaffolds for tissue engineering. In the present study different surface treatments were evaluated as modulators of biomaterial–cell adhesion. The surface morphology and topography were affected by the induced modifications. Higher surface roughness measurements were obtained for the modified membranes, with significantly higher effects observed on alkali-treated samples. The treatments applied had significantly greater effects on the final mechanical performance of samples analysed in the hydrated state as a result of the water absorption by the polymeric fibres. The surface free energy was higher after the applied surface treatments and the incorporation of oxygen-containing groups, as a result of the chemical/physical modifications. The effect of the surface properties modification on the adhesion and morphology of fibroblasts was further investigated. Greater number of cells adhered to the modified textile surfaces after short culture periods and a different cell morphology was observed depending on the treatment applied. By analysing the surface parameters studied, the roughness induced by the surface treatments stimulated cell adhesion and the increased hydrophilicity also favoured such behaviour. Nevertheless, it was not possible to obtain a direct relationship between cell adhesion and the physical/chemical surface properties obtained after each modification. The effects of each treatment on cell behaviour may be more pronounced and distinctive after longer culture periods, particularly on those treatments that affected the bulk properties of the materials, such as the NaOH treatment, for which an increase in the degradation rate is expected. The plasma treatment conditions (concentration of monomer and etching time) led to a very thin polymer layer on the substrate. Therefore, the delamination process is not expected to be a long-term effect. Nevertheless, longer degradation studies need to be performed in order to assess the stability of the surface. Overall, the possibility of applying these treatments to modulate the surface properties of complex 3D scaffolds make the methods reported attractive for further investigations as part of a TE processing route.

Acknowledgments

The authors acknowledge the Portuguese Foundation for Science and Technology (FCT) under POCTI and/or FEDER programmes under the scope of the project TISSUE2TISSUE (PTDC/CTM/105703/2008). The FCT distinction attributed to ALO under the Investigator FCT programme (IF/00411/2013) is also gratefully acknowledged.

Conflict of interest

The authors have declared that there is no conflict of interest.

DOI: 10.1002/term

References

Almeida LR, Martins AR, Fernandes EM, *et al*. 2013; New biotextiles for tissue engineering: Development, characterization and *in vitro* cellular viability. *Acta Biomater* **9**: 8167–8181.

Altman GH, Diaz F, Jakuba C, *et al*. 2003; Silk-based biomaterials. *Biomaterials* **24**: 401–416.

Anselme K. 2000; Osteoblast adhesion on biomaterials. *Biomaterials* **21**: 667–681.

Bullett NA, Bullett DP, Truica-Marasescu FE, *et al*. 2004; Polymer surface micropatterning by plasma and VUV-photochemical modification for controlled cell culture. *Appl Surf Sci* **235**: 395–405.

Burns JP, Snyder SJ. 2009; Biologic patches for management of irreparable rotator cuff tears. *Techn Shoulder Elbow Surg* **10**: 11–21.

Chan CM. 1994; Contact angle measurement. In Polymer Surface Modification and Characterization, (CM Chan ed.). Verlag CH, Hanser Publishers: Munich, 285.

Chen JP, Su CH. 2011; Surface modification of electrospun PLLA nanofibers by plasma treatment and cationized gelatin immobilization for cartilage tissue engineering, *Acta Biomater* **7**: 234–243.

Chen M, Patra PK, Lovett ML, *et al*. 2009; Role of electrospun fibre diameter and corresponding specific surface area (SSA) on cell attachment. *J Tissue Eng Regen Med* **3**: 269–279.

Cho K, Lee J, Kwon K. 2001; Hydrolytic degradation behavior of poly (butylene succinate) with different crystalline morphologies. *J Appl Polym Sci* **79**: 1025–1033.

Correlo VM, Boesel LF, Bhattacharya M, *et al*. 2005, Properties of melt processed chitosan and aliphatic polyester blends. *Mater Sci Eng A Struct Mater* **403**: 57–68.

Correlo VM, Costa-Pinto AR, Sol P, *et al*. 2010; Melt processing of chitosan-based fibers and fiber-mesh scaffolds for the engineering of connective tissues. *Macromol Biosci* **10**: 1495–1504.

Coutinho DF, Pashkuleva IH, Alves CM, *et al*. 2008; The effect of chitosan on the *in vitro* biological performance of chitosan-poly(butylene succinate) blends. *Biomacromolecules* **9**: 1139–1145.

Craighead HG, James CD, Turner AMP. 2001; Chemical and topographical patterning for directed cell attachment. *Curr Opin Solid St M* **5**: 177–184.

Declercq HA, Desmet T, Berneel EE, *et al*. 2013; Synergistic effect of surface modification and scaffold design of bioplotted 3-D poly-ε-caprolactone scaffolds in osteogenic tissue engineering. *Acta Biomater* **9**: 7699–7708.

Delaittre G, Greiner AM, Pauloehrl T, *et al*. 2012; Chemical approaches to synthetic polymer surface biofunctionalization for targeted cell adhesion using small binding motifs. *Soft Matter* **8**: 7323–7347.

Dhakal H, Zhang Z, Richardson M. 2007; Effect of water absorption on the mechanical properties of hemp fibre reinforced unsaturated polyester composites. *Compos Sci Technol* **67**: 1674–1683.

Ellison M, Fisher L, Alger K, *et al*. 1982; Physical properties of polyester fibers degraded by aminolysis and by alkalin hydrolysis. *J Appl Polym Sci* **27**: 247–257.

Fan HB, Liu HF, Toh SL, *et al*. 2009; Anterior cruciate ligament regeneration using mesenchymal stem cells and silk scaffold in large animal model. *Biomaterials* **30**: 4967–4977.

Fujimaki T. 1998; Processability and properties of aliphatic polyesters, 'BIONOLLE', synthesized by polycondensation reaction. *Polym Degrad Stab* **59**: 209–214.

Gao JM, Niklason L, Langer R. 1998; Surface hydrolysis of poly(glycolic acid) meshes increases the seeding density of vascular smooth muscle cells. *J Biomed Mater Res* **42**: 417–424.

Gomes ME, Holtorf HL, Reis RL, Mikos AG. 2006; Influence of the porosity of starch-based fiber mesh scaffolds on the proliferation and osteogenic differentiation of bone marrow stromal cells cultured in a flow perfusion bioreactor. *Tissue Eng* **12**: 801–809.

Hutmacher DW. 2000; Scaffolds in tissue engineering bone and cartilage. *Biomaterials* **21**: 2529–2543.

Inui A, Kokubu T, Makino T, *et al*. 2010; Potency of double-layered poly L-lactic acid scaffold in tissue engineering of tendon tissue. *Int Orthop* **34**: 1327–1332.

Kaelble DH. 1970; Dispersion-polar surface tension properties of organic solids. *J Adhesion* **2**: 66–81.

Kim HS, Kim HJ, Lee JW, *et al*. 2006; Biodegradability of bio-flour filled biodegradable poly(butylene succinate) bio-composites in natural and compost soil. *Polym Degrad Stab* **91**: 1117–1127.

Li GH, Liu H, Li TD, *et al*. 2012; Surface modification and functionalization of silk fibroin fibers/fabric toward high performance applications. *Mater Sci Eng C Mater Biol Appl* **32**: 627–636.

Li HY, Chang J, Cao AM, *et al*. 2005; *In vitro* evaluation of biodegradable poly(butylene succinate) as a novel biomaterial. *Macromol Biosci* **5**: 433–440.

Lim JY, Donahue HJ. 2007; Cell sensing and response to micro- and nanostructured surfaces produced by chemical and topographic patterning. *Tissue Eng* **13**: 1879–1891.

Liu CZ, Shen SZ, Han ZW. 2011; Surface wettability and chemistry of ozone perfusion processed porous collagen scaffold. *J Bionic Eng* **8**: 223–233.

Liu HF, Fan HB, Wang Y, *et al*. 2008; The interaction between a combined knitted silk scaffold and microporous silk sponge with human mesenchymal stem cells for ligament tissue engineering. *Biomaterials* **29**: 662–674.

Liu LF, Yu JY, Cheng LD, *et al*. 2009; Mechanical properties of poly(butylene succinate) (PBS) biocomposites reinforced with surface modified jute fibre. *Compos Part A Appl Sci Manuf* **40**: 669–674.

Liu ZT, Zhang XL, Jiang Y, *et al*. 2010; Four-strand hamstring tendon autograft versus LARS artificial ligament for anterior cruciate ligament reconstruction. *Int Orthop* **34**: 45–49.

Lopez-Perez PM, da Silva RMP, Sousa RA, *et al*. 2010; Plasma-induced polymerization as a tool for surface functionalization of polymer scaffolds for bone tissue engineering: an *in vitro* study. *Acta Biomater* **6**: 3704–3712.

Martins A, Gang W, Pinho ED, *et al*. 2010; Surface modification of a biodegradable composite by UV laser ablation: *in vitro* biological performance. *J Tissue Eng Regen M* **4**: 444–453.

Mitchell SA, Davidson MR, Bradley RH. 2005; Improved cellular adhesion to acetone plasma modified polystyrene surfaces. *J Colloid Interface Sci* **281**: 122–129.

Oliveira AL, Malafaya PB, Costa SA, *et al*. 2007; Micro-computed tomography (micro-CT) as a potential tool to assess the effect of dynamic coating routes on the formation of biomimetic apatite layers on 3D-plotted biodegradable polymeric scaffolds. *J Mater Sci Mater Med* **18**: 211–223.

Oliveira JT, Correlo VM, Sol PC, *et al*. 2008; Assessment of the suitability of chitosan/polybutylene succinate scaffolds seeded with mouse mesenchymal progenitor cells for a cartilage tissue engineering approach. *Tissue Eng Part A* **14**: 1651–1661.

Park K, Ju YM, Son JS, *et al*. 2007; Surface modification of biodegradable electrospun nanofiber scaffolds and their interaction with fibroblasts. *J Biomater Sci Polym Ed* **18**: 369–382.

Pashkuleva I, Reis RL. 2004; Surface activation and modification – a way for improving the biocompatibility of degradable biomaterials. In *Biodegradable Systems in Medical Functions*: *Design Processing Testing and Application* (RL Reis, JS Roman eds.). CRC press: Boca Raton, FL, 429–454.

Pashkuleva I, Azevedo HS, Reis RL. 2008; Surface structural investigation of starch-based biomaterials. *Macromol Biosci* **8**: 210–219.

Pashkuleva I, Marques AP, Vaz F, *et al*. 2010; Surface modification of starch based biomaterials by oxygen plasma or UV-irradiation. *J Mater Sci Mater Med* **21**: 21–32.

Phua YJ, Lau NS, Sudesh K, *et al*. 2012; Biodegradability studies of poly(butylene succinate)/organo-montmorillonite nanocomposites under controlled compost soil conditions: effects of clay loading and compatibiliser. *Polym Degrad Stab* **97**: 1345–1354.

Ramakrishna S. 2001; Textile scaffolds in tissue engineering. In Smart Fibres Fabrics and Clothing (X Tao ed.). Woodhead Publishing, CRC Press: Cambridge, 291–313.

Ratner BD. 1996; Surface properties of materials. In *Biomaterials Science*: *an Introduction to Materials in Medicine* (BD Ratner, A Hoffman, F Schoen *et al*. eds). Academic Press: New York, NY, 21.

Safinia L, Wilson K, Mantalaris A, *et al*. 2007; Atmospheric plasma treatment of porous polymer constructs for tissue engineering applications. *Macromol Biosci* **7**: 315–327.

Salgado AJ, Coutinho OP, Reis RL. 2004; Bone tissue engineering: state of the art and future trends. *Macromol Biosci* **4**: 743–765.

Shikinami Y, Kawabe Y, Yasukawa K, *et al*. 2010; A biomimetic artificial intervertebral disc system composed of a cubic three-dimensional fabric. *Spine J* **10**: 141–152.

Stevens MM, George JH. 2005; Exploring and engineering the cell surface interface. *Science* **310**: 1135–1138.

Sumanasinghe R, King MW. 2003; New trends in biotextiles – the challenge of tissue engineering. *J Text Apparel Technol Manage* **3**: 1–13.

Sumanasinghe R, King MW. 2005; The applications of biotextiles in tissue engineering. *J Text Apparel Technol Manage* **9**: 80–90.

Tuzlakoglu K, Reis RL. 2009; Biodegradable polymeric fiber structures in tissue engineering. *Tissue Eng Part B Rev* **15**: 17–27.

Wang S, Zhang Y, Wang H, *et al*. 2011; Preparation, characterization and biocompatibility of electrospinning heparin-modified silk fibroin nanofibers, *Int J Biol Macromol* **48**: 345–353.

Wang X, You C, Hu X, *et al*. 2013; The roles of knitted mesh-reinforced collagen-chitosan hybrid scaffold in the one-step repair of full-thickness skin defects in rats. *Acta Biomater* **9**: 7822–7832.

Wenzel RN. 1936; Resistance of solid surfaces to wetting by water. *Ind Eng Chem* **28**: 988–994.

Yoo HS, Kim TG, Park TG. 2009; Surface-functionalized electrospun nanofibers for tissue engineering and drug delivery. *Adv Drug Deliv Rev* **61**: 1033–1042.

Zanden C, Voinova M, Gold J, *et al*. 2012; Surface characterisation of oxygen plasma treated electrospun polyurethane fibres and their interaction with red blood cells. *Eur Polym J* **48**: 472–482.

Zeronian SH, Collins MJ. 1989; Surface modification of polyester by alkaline treatments. *Text Prog* **20**: 1–26.

Zhao HP, Zhu JT, Fu ZY, *et al*. 2008; Plasma surface graft of acrylic acid and biodegradation of poly(butylene succinate) films. *Thin Solid Films* **516**: 5659–5663.

Supporting information

Additional supporting information may be found in the online version of this article at the publisher's web-site.

Figure S1. XPS survey spectrum of untreated PBS.
Figure S2. XPS survey spectrum of PBS grafted with VPA. The inset represents higher magnification of the part of spectrum where the P peaks appear in comparison with the same portion of the spectrum of untreated PBS.
Figure S3. P2p core level spectra of VPA-grafted PBS.
Figure S4. S2p core level spectra of VSA-grafted PBS.

DOI: 10.1002/term